Applied Catalysis A: General 458 (2013) 82–89

Contents lists available at SciVerse ScienceDirect

Applied Catalysis A: General

journal homepage: www.elsevier.com/locate/apcata

Enhanced catalytic performance for SiO_2–TiO_2 binary oxide supported Cu-based catalyst in the hydrogenation of dimethyloxalate

Chao Wen[a], Anyuan Yin[a], Yuanyuan Cui[a], Xinli Yang[b], Wei-Lin Dai[a,*], Kangnian Fan[a]

[a] Department of Chemistry and Shanghai Key Laboratory of Molecular Catalysis and Innovative Materials, Fudan University, Shanghai 200433, PR China
[b] College of Chemistry & Chemical Engineering, Henan University of Technology, Zhengzhou 450001, Henan, China

ARTICLE INFO

Article history:
Received 9 December 2012
Received in revised form 11 March 2013
Accepted 16 March 2013
Available online xxx

Keywords:
Binary-oxide support
Dimethyloxalate hydrogenation
Ethylene glycol
Cu/SiO_2–TiO_2

ABSTRACT

Copper based catalyst with Si–Ti binary-oxide support is synthesized via a facile ammonia evaporation method for selective hydrogenation of dimethyloxalate (DMO) to ethylene glycol (EG). 100% conversion of DMO and 90% selectivity to EG could be obtained over the Cu/SiO_2–TiO_2 catalyst at high liquid hourly space velocity (LHSV). Catalytic stability is greatly enhanced when the Si–Ti binary oxide is used as support because of the intimate interaction between copper species and the support. The improved catalytic performance compared to the unitary oxide-supported catalysts SiO_2 and TiO_2 could be attributed to the highly dispersed copper species stabilized by the binary support. Also, the electron transfer from TiO_2 to Cu-species is found to play an important role in improving the surface charge density of the metallic copper, which is helpful to improve the catalytic activity.

1. Introduction

Ethylene glycol (EG), as one of the most important industrial chemicals, is widely used in various applications, such as antifreeze, polyester fibers, alkyd resin in polyester manufacture, and solvents [1]. Current production for EG is based on the hydrolysis of ethylene oxide obtained by direct oxidation of ethylene with air or oxygen (petroleum-derived EG) [2]. However, due to the long-term shortage and increased price of crude oil as well as an increasing demand for EG, an intensive exploration for producing organic intermediates from C1 units has significant influence on the EG synthesis. One of the synthesis processes now arousing great interests is hydrogenation of dimethyloxalate (DMO) to EG, which includes two steps: the coupling of CO with nitrite esters to oxalates, then hydrogenation of oxalates to EG. Considerable works have been devoted to the hydrogenation of oxalates since the 1970s and Cu-based heterogeneous catalysts have been improved to exhibit outstanding catalytic performance in the hydrogenation of DMO to EG [3–5].

Cu/SiO_2 catalysts have been extensively applied in various reactions, especially for the hydrogenation process [6–8]. On account of cupreous active sites for the selective hydrogenation of carbon–oxygen bonds and relatively inactive for the hydrogenolysis of carbon–carbon bonds [9], and the moderate acidic and basic properties of SiO_2 as support [10], Cu/SiO_2 catalyst exhibits outstanding catalytic activity and selectivity in hydrogenation of DMO to EG [11–15]. The proper dispersion of copper active sites on silica supports is one of the crucial factors for the catalytic performance and stability of the catalyst [16]. However, in Cu/SiO_2 catalysts, the copper particles tend to aggregate under elevated reaction temperature due to the weak interaction between copper species and the SiO_2 support, which decrease their catalytic performance drastically. Taking this result into consideration, to fabricate a catalyst with high stability as well as highly dispersed copper species is one of the great challenges not only for academic research but also for industrial application.

Substantial studies have been done to probe the relationship between the catalytic performance and the interaction of the active sites with supports in the copper based catalysts. As we know, electron transfer always occurs between active sites and the supports. Irie et al. [17,18] studied the Cu (II)-grafted TiO_2 catalyst, and found the electrons in the valence band of TiO_2 were directly transferred to Cu (II), as well as holes in the valence band of TiO_2, which leaded to the excellent catalytic activity and stability. They suggested that copper was more inclined to interact with metal oxides than the nonmetal oxides. Fujitani and co-workers [19,20] studied the specific activities of methanol synthesis compared with Cu/SiO_2 and $Cu/ZnO/SiO_2$ and considered that ZnO_x moieties formed by the reduction process at high temperature migrated on the surface of Cu particles and dissolved into the bulk of copper to form Cu–Zn alloy which enhanced the catalytic activity greatly. They inferred that the new active site generated by ZnO_x moieties can be thought as an analogous strong metal support interaction (SMSI) [21].

A lot of investigations have been done to study the copper based binary oxide supports. It is accepted that catalysts

* Corresponding author. Tel.: +86 5566 4678; fax: +86 5566 5572.
E-mail address: wldai@fudan.edu.cn (W.-L. Dai).

0926-860X/$ – see front matter © 2013 Elsevier B.V. All rights reserved.
http://dx.doi.org/10.1016/j.apcata.2013.03.021

using binary oxide as supports exhibits more attractive properties such as mechanical strength, thermal stability and larger surface area. Binary SiO_2–TiO_2 used as catalyst in the selective oxidation reactions presented superb activity which was regarded as the generation of new catalytic sites [22,23]. However, the preparation of the catalyst is complicated, and usually requires organic solvents and surfactant which are always harmful to the environment. Boccuzzi et al. [24,25] studied the Cu/SiO_2 and Cu/SiO_2–TiO_2 catalysts in a polymerization reaction and found that morphological and surface properties of the copper phase were essentially the same for all the catalysts investigated. An intriguing observation was that the TiO_2 phase presented in Cu/SiO_2–TiO_2 formed TiO_x suboxides and covered a fraction of the exposed Cu metal sites by reduction at higher temperature. They also observed the electron transfer from TiO_2 to Cu directly, which can be interpreted as the strong interactions between copper and titanium. Although using binary oxide as support can improve the catalytic property in many different aspects, few attempts have been done to investigate the interaction between the active sites and the binary oxide supports. Furthermore, the application scope for catalysts with binary oxide support is still scarce; there are few reports of the applications in the hydrogenation reactions especially for the ester hydrogenation.

Ground on the above discussions, it is expected that the copper based catalyst with Si–Ti binary-oxide support may exhibit intimate interaction between copper species and the supports, and the electronic interaction between copper and titanium will accommodate the texture of the catalyst and further enhance the catalytic performance. In our previous study, hydrogenation of DMO is systematically investigated based on the Cu/SiO_2 catalysts and a high yield of EG can be obtained under optimized conditions [11–15]. However, it is easy to deactivate especially for the long-term running due to the poor interaction between copper and silica [26]. In addition, to the best of our knowledge, most of the catalysts used in this reaction are based on unitary SiO_2 as support which shows low mechanical strength and poor stability in alkaline environment. These drawbacks greatly restrict its industrial application. Herein, we fabricate a high-efficient and stable catalyst with a novel Si–Ti binary oxide as support in selective hydrogenation of DMO to EG in an attempt to investigate the enhancement mechanism in the catalytic performance caused by the binary oxide support.

2. Experimental

2.1. Catalyst preparation

All the reagents are purchased from Sinopharm Chem. Reagent Co., Ltd. without further purification, unless otherwise specified.

To obtain the Si–Ti binary oxide support, a titania sol is synthesized via a facile method. Firstly, 10 ml of $Ti(OBu)_4$ is added into 30 ml of ethanol solution which contains 2 ml of acetic acid and the solution is kept magnetic stirring for 0.5 h. Then, small amount of nitric acid is added to control the pH value below 3.0. Finally, 10 ml of ethanol and 1 ml of deionized water are added to the solution and the TiO_2 sol are obtained after the mixture was kept stirring for 1 h.

The Cu/SiO_2–TiO_2 catalyst precursor with 10 wt.% copper loadings and Si/Ti molar ratio of 3:1 is prepared by ammonia evaporation method (AE) [27]. Firstly, 1.9 g of $Cu(NO_3)_2{\cdot}3H_2O$ are dissolved into 100 ml of deionized water, then, about 11 ml of aqueous ammonia (25 wt.%) are added to the above solution and the pH is adjusted to 11.0. After that, mixed sols containing 12 ml of silica sol (JN30, Qingdao Haiyang Chem. Co., Ltd.) and 15 ml of titania sol containing 1.25 g of TiO_2 are added dropwise into the solution. The as-obtained suspensions are kept stirring for 2 h at room temperature, and then the temperature is risen to 363 K to decompose the cuprammonia until the pH value reached 6–7. After then, the filtrate is washed with deionized water for five times and dried at 393 K overnight. Finally, the catalyst precursors are calcined in static air at 723 K for 4 h, then pelletized, and grounded to 40–60 meshes. For comparison, Cu/SiO_2 and Cu/TiO_2 both containing 10 wt.% Cu are synthesized using the similar method as Cu/SiO_2–TiO_2 without the addition of titania-sol or silica-sol, respectively. All the catalyst precursors are then reduced at 573 K for 4 h under the 5% H_2/Ar (v/v) atmosphere.

2.2. Catalyst characterization

Specific surface areas of the catalysts are measured by nitrogen adsorption–desorption method at 77 K (Micromeritics Tristar ASAP 3000) using Brunauer–Emmett–Teller (BET) method. The copper loadings are determined by the inductively coupled plasma method (ICP, thermo E.IRIS). The wide-angle XRD patterns were collected on a Bruker D8 Advance X-ray diffractometer using nickel-filtered Cu Kα radiation (λ = 0.15406 nm) with a scanning angle (2θ) range of 20–90°, a scanning speed of 2° min^{-1}, and a voltage and current of 40 kV and 40 mA, respectively. TEM micrographs are obtained on a JOEL JEM 2010 transmission electron microscope. Temperate programmable reduction (TPR) profiles were obtained on a Tianjin XQ TP5080 auto-adsorption apparatus. 30 mg of the calcinated catalyst was outgassed at 473 K under Ar flow for 2 h. After cooling to room temperature under Ar flow, the in-line gas was switched to 5% H_2/Ar (v/v), and the sample was heated to 773 K at a ramping rate of 10 K min^{-1}. The H_2 consumption was monitored by a TCD detector. The metallic Cu surface area was measured by decomposition of N_2O at 323 K using a pulsed method with N_2 as the carrier gas. The consumption of N_2O was detected also by a TCD detector. The specific area of metallic copper was calculated from the total amount of N_2O consumption with 1.46×10^{19} copper atoms per m^2 [28]. X-ray photoelectron spectroscopy (XPS) was recorded with a Perkin Elmer PHI 5000 C ESCA system equipped with a hemispherical electron energy analyzer. The Mg-Kα (1253.6 eV) anode was operated at 14 kV and 20 mA. The carbonaceous C 1s line (284.6 eV) was used as the reference to calibrate the binding energies (BEs).

2.3. Activity measurements.

The catalytic activity test was conducted using a fixed-bed reactor. Typically, 2.0 g of catalyst (40–60 meshes) sample was packed into a stainless steel tubular reactor (i.d., 10 mm) with the thermocouple inserted into the catalyst bed for better control of the actual pretreatment and reaction temperature. Catalyst activation was performed at 573 K for 4 h with a ramping rate of 2 K min^{-1} from the room temperature. After cooling to the reaction temperature, 15 wt.% of DMO (purity > 99%) in methanol and H_2 were fed into the reactor at a H_2/DMO molar ratio of 100 and a system pressure of 3.0 MPa. The reaction temperature was first set at 473 K and the LHSV of DMO was set in the range from 0.15 to 0.8 h^{-1}. The products were condensed, and analyzed on a gas chromatograph (Finnigan Trace GC ultra) fitted with an AT.FFAP capillary column and a flame ionization detector (FID).

3. Results

3.1. Structural and textural properties

The textural properties and the chemical compositions of the three catalysts are listed in Table 1. The BET surface area of Cu/TiO_2 is only 48 m^2 g^{-1}, much smaller than that of Cu/SiO_2. When the Si–Ti binary oxide is used as support, the catalyst shows a large specific surface area, 238 m^2 g^{-1}, and an average pore volume of 0.4 cm^3 g^{-1}. It is interesting to find that the specific surface area

Table 1
The textural properties and chemical compositions of the catalysts.

	Cu loading[a] (wt.%)	S_{BET} ($m^2\ g^{-1}$)	D_{pore} (nm)	V_{pore} (cm^3)	S_{Cu}[b] ($m^2\ g^{-1}_{catal}$)	BE_{Cu}[c] (eV)	BE_{Cu}[d] (eV)	BE_{T}[c] $_{i}$(eV)	BE_{Ti}[d] (eV)
Cu/SiO_2	9.6	294	12.6	1.2	7.8	933.2	932.2	–	–
Cu/TiO_2	9.8	48	27.9	0.4	5.4	933.4	932.6	458.5	457.7
Cu/SiO_2–TiO_2	9.7	238	5.7	0.5	8.2	933.6	932.0	457.9	457.8

[a] Metal loading determined by ICP.
[b] Cu metal surface area determined by N_2O titration method.
[c] Binding energy (Cu 2p3/2) of the calcinated samples.
[d] Binding energy (Cu 2p3/2) of the reduced samples.

of Cu/SiO_2–TiO_2 is near that of Cu/SiO_2, whose value is about 294 $m^2\ g^{-1}$, indicating that the textural structure of the two catalysts is similar. The results of the metallic Cu surface area (S_{Cu}) measured by N_2O titration method are shown in Table 1. The Cu/TiO_2 catalyst exhibits the smallest metallic Cu surface area (S_{Cu}), while the S_{Cu} of Cu/SiO_2–TiO_2 and Cu/SiO_2 is similar, which indicates that the introduction of TiO_2 into the binary oxide support has no side impact on the dispersion of the copper species [29].

The XRD characterizations of the three catalysts calcinated at 623 K are shown in Fig. 1A. No obvious diffraction peaks for Cu/SiO_2–TiO_2 could be observed, indicating that the SiO_2 and TiO_2 present as an amorphous state. In addition, no diffraction peaks from cupric oxide or any related cupreous substances could be detected in the Cu/SiO_2 and Cu/SiO_2–TiO_2 samples, suggesting that copper species are highly dispersed on these supports. However, two diffraction peaks in the proximity of $2\theta = 36.5^\circ$ and 42.4° characteristic of CuO (JCPDS 44-0706) are observed for Cu/TiO_2, pointing out that copper oxide species are more inclined to aggregate into large particles. The poor specific surface area of the TiO_2 may be responsible for the aggregation of copper oxide species. Fig. 1B presents the XRD patterns obtained for the reduced catalysts. The appearance of the peaks from Cu(1 1 1), Cu(2 0 0) and Cu(2 2 0) diffraction peaks (JCPDS 01-1241) can be distinguished easily. It is obvious to find that the metallic copper diffraction peaks in the Cu/TiO_2 are sharper and stronger than those in the other two catalysts. This finding suggests the particle size of the copper species is much larger on the Cu/TiO_2. Generally speaking, the interaction between the metallic copper and metal oxide support seems to be stronger than that of copper to nonmetal oxide support, however, the specific surface area is another crucial factor to influence the metal dispersion. Poor specific surface area resulting in the aggregation of metal particles has been reported a lot, for instance, Xin et al. [30] studied the Nafion® ionomer aggregation and found that the poor dispersion of Pt particles in the $S-1$ sample was mainly caused by the smaller specific surface area of the catalyst layer. Thus, the low S_{BET} value seems to be a major factor for the poor dispersion of copper particles in the Cu/TiO_2 catalyst. Another finding is that parts of the anatase phase transforms into rutile phase after heat treatment with H_2. In addition, a diffraction peak at $2\theta = 36.8^\circ$ attributed to Cu_2O phase (JCPDS 34-1354) is also observed in the sample of Cu/SiO_2, indicating that the reduction of Cu^{2+} species upon H_2-reduction is not completed in Cu/SiO_2.

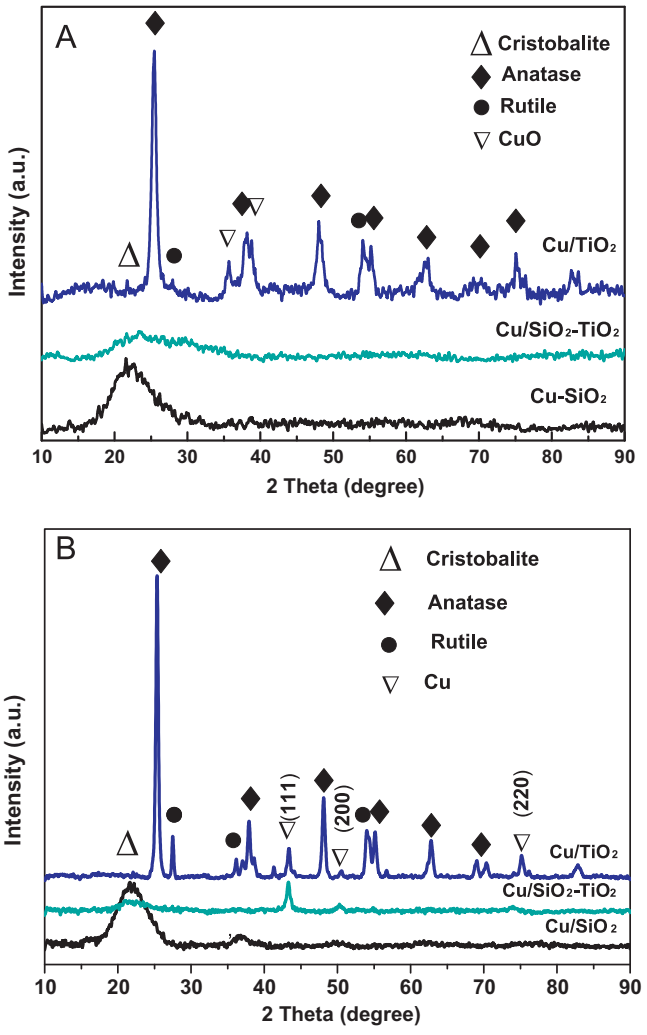

Fig. 1. (A) XRD patterns of the three catalysts after calcinated at 723 K and (B) after reduced at 573 K.

Fig. 2 shows the TEM images of the reduced catalysts. For the Cu/SiO_2 shown in Fig. 2A, the metallic particles are dispersed uniformly on the SiO_2 supports, and there is no agglomeration of copper species condensed on SiO_2. The high dispersion can be attributed to the relatively larger specific surface area of SiO_2 that provides favorable dispersing effect for the copper species. However, the copper particles in Cu/TiO_2 shown in Fig. 2B present in large particle size and nonuniform size distribution. The sintering and aggregation of the active species can be thought as the results of the low specific surface area of the support. Fig. 2C and D shows the TEM images of the reduced Cu/SiO_2–TiO_2 with different plotting scale. The copper species homogeneously disperse throughout the spherical supports and it is hard to distinguish between the SiO_2 and TiO_2, implying that the Ti and Si species are completely mixed together which accords well with the XRD characterizations.

3.2. Redox behaviors

TPR characterization is carried out to investigate the redox properties of the copper based catalysts. The results are shown in Fig. 3. A dominant peak at 522 K with a shoulder peak at 533 K can be picked out in Cu/SiO_2. Previous studies suggest that the peaks at temperatures higher than 523 K can be assigned to the reduction of

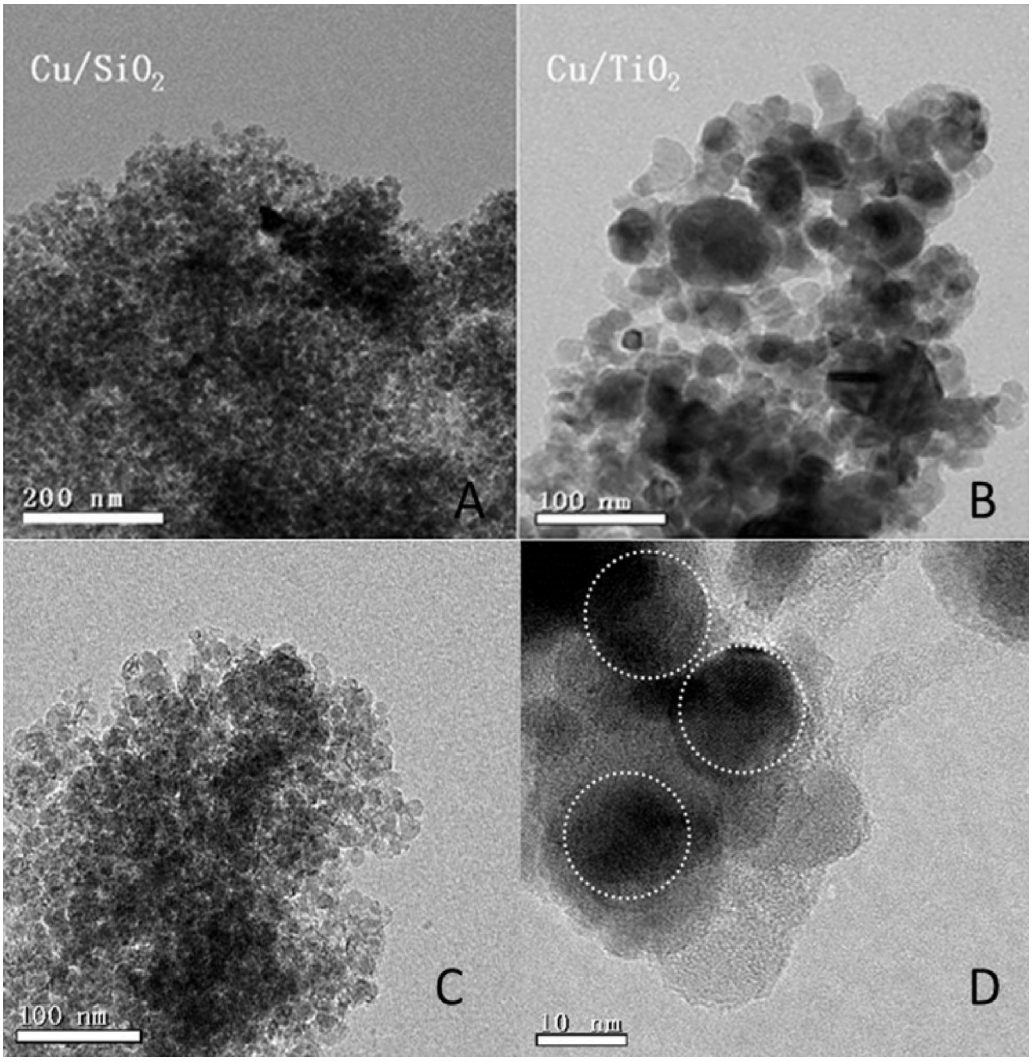

Fig. 2. TEM images of the three catalysts: (A) Cu/SiO_2, (B) Cu/TiO_2, (C) and (D) Cu/SiO_2–TiO_2.

the copper oxide crystal phase [31,32]. Thus, there must be certain amount of copper species in the form of bulk CuO on the silica support. The shoulder peak at 533 K can be ascribed to the reduction of copper phyllosilicate generated during the calcination process.

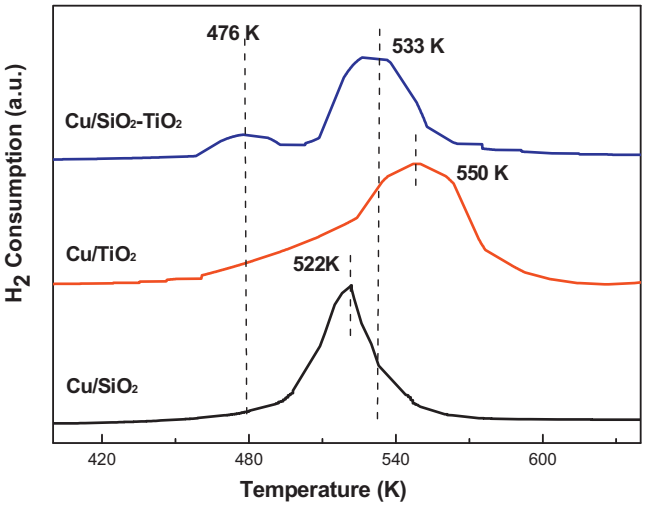

Fig. 3. TPR profiles of the catalysts.

The Cu/TiO_2 sample shows an asymmetric and broad peak at 550 K due to the strong interaction between copper oxide species and the TiO_2 support. It is worth noting that the growing hydrogen consumption can be observed because of the reduction of well dispersed copper species when the temperature reaches 476 K. This observation can be understood by taking into consideration that TiO_2 is an n-type semiconductor. Under a reducing atmosphere, TiO_2 tends to produce a high concentration of n-type defect, i.e. unstable Ti^{3+} ions and oxygen vacancies on the surface, and by donating electric charges to the copper species, the Ti^{3+} recovers to Ti^{4+}, and the reduction capacity of copper oxide species is promoted [33]. This result can also be thought as a direct evidence for the electron transfer from titanium to copper species on the interface. However, the small specific surface area of titanium and the poor dispersion of copper species seriously restrict the copper oxide reduction, thus the Cu/TiO_2 catalyst exhibits a main reduction peak at higher temperature. The TPR profile of Cu/SiO_2–TiO_2 catalyst displays two detached peaks at 477 and 531 K, indicating that there are at least two different copper species in the sample. The lower temperature peak may be assigned to the reduction of highly dispersed CuO species [27] and some copper species with surface electrons enriched caused by TiO_2. Thus, the well dispersed copper oxide species and the obvious beneficial influence of TiO_2 as well as the lower reduction temperature could be obtained by using Si–Ti binary oxide support.

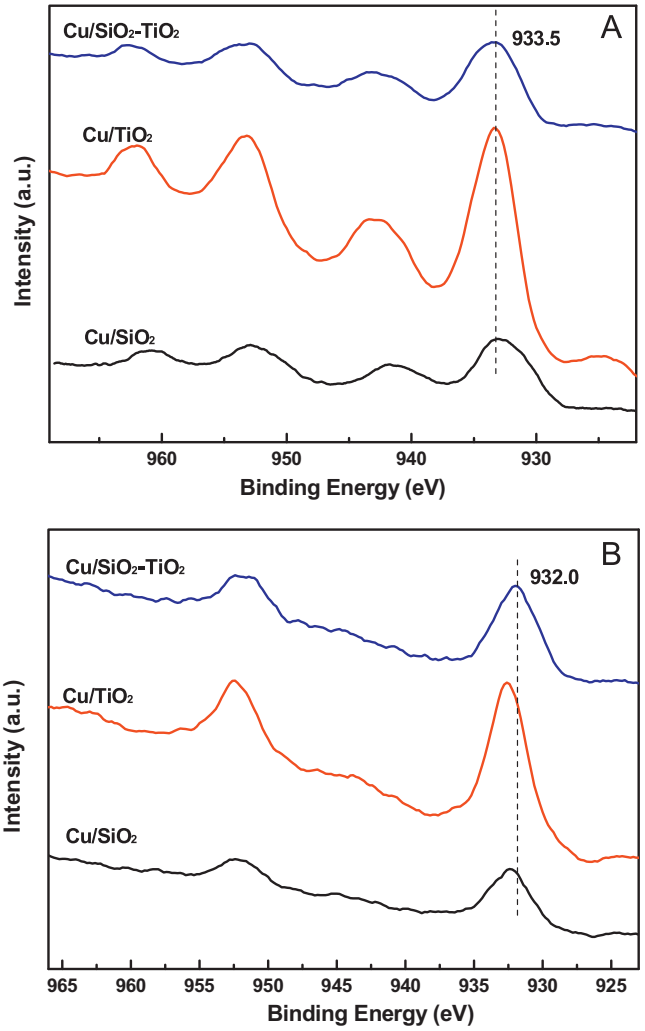

Fig. 4. (A) Cu 2p XPS spectra of the calcinated catalysts and (B) the reduced catalysts.

3.3. Chemical state and surface composition

The Cu $2p_{3/2}$ XPS results of the calcinated catalysts are shown in Table 1 and Fig. 4, and the binding energy of Cu $2p_{3/2}$ peak at above 933.5 eV along with the presence of the characteristic shakeup satellite peaks suggests that the copper oxidation state is +2. Besides, the BEs of Cu/SiO_2 for Cu $2p_{3/2}$ present a slower blue shift compared with those of Cu/TiO_2 and Cu/SiO_2–TiO_2, indicating the weaker interaction between the copper oxide and the silica supports. Fig. 4B shows the Cu 2p X-ray photoelectron spectra of the reduced catalysts. The BEs of Cu $2p_{3/2}$ in Cu/TiO_2 is much higher than that of Cu/SiO_2, indicating that the copper species are more inclined to interact with metal oxide substrate. As we know, the increase in BE of an element is the consequence of the increase in the effective positive charge on it [34]. Therefore, the outer shell electronic density of the reduced copper species in Cu/TiO_2 is lower than that of Cu/SiO_2. This result can explain why the copper oxide in Cu/TiO_2 is much more difficult to be reduced under identical conditions. However, it is worth to mention that the Cu $2p_{3/2}$ BEs in the reduced Cu/SiO_2–TiO_2 are lower than those in the other two catalysts, indicating that there may be more negative charges on the surface of copper species. It is interesting to find that much higher intensity of Cu 2p and Cu LMM XP spectra in Cu/TiO_2 than the other two samples are observed, which can be ascribed to the evenness and cleanness of the TiO_2 sample. However, the higher crystallinity

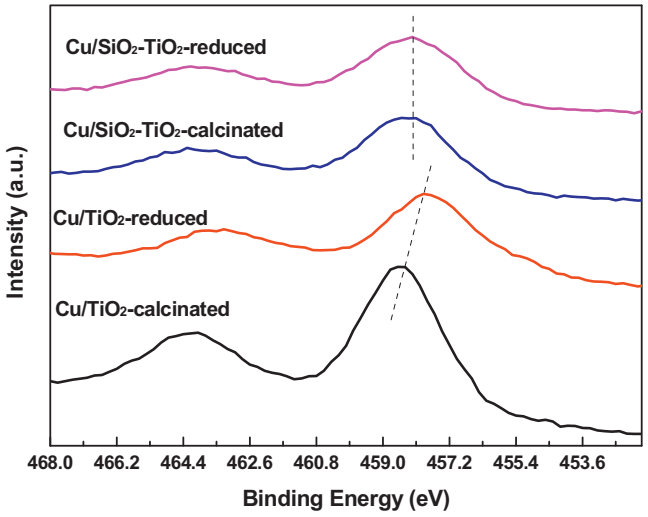

Fig. 5. Ti 2p XPS spectra of the catalysts after calcinated at 723 K and reduced at 573 K.

of TiO_2 and the much higher BET area of SiO_2 and SiO_2–TiO_2 all contribute to this phenomenon.

The XPS spectra of Ti $2p_{3/2}$ in the calcinated and reduced catalysts are displayed in Fig. 5. The fact that Ti $2p_{3/2}$ core level appears at 458.3 eV in the calcinated Cu/SiO_2–TiO_2 confirms the formation of the Ti–O–Si hetero linkages [35], suggesting that the titanium is strongly bonded to the silica framework [36]. It is interesting to find that, after the reduction process, the BE of Ti $2p_{3/2}$ in the Cu/TiO_2 sample decreased from 458.5 to 457.7 eV, whereas this value in the Cu/SiO_2–TiO_2 retains constant. This phenomenon can be explained according to the following considerations. The electrons in the narrow band energy of TiO_2 are easy to excite from the valance band to the conductive band at the higher temperature under reduction atmosphere [37], thus, during the reduction process, there must be certain amount of Ti^{4+} in the TiO_2 support could be reduced to Ti^{3+} and cause decrease in BEs. However, in the Cu/SiO_2–TiO_2 sample, which the copper species disperse uniformly on the homogeneous mixture of Si–Ti oxide, once Ti^{4+} captures one electron and is reduced to Ti^{3+}, the mobile electrons will be transferred to neighboring Cu on the interface immediately and Ti^{3+} recovers to Ti^{4+}, so the valence state of titanium do not change. In other words, the electron transfer from Ti^{4+} to Cu definitely occurs during the reduction condition and further lead to more native charges on the copper surface with the blue shift in BEs of Cu $2p_{3/2}$. Goodenough et al. [38] studied the Pt–Ru electrodes and found that the Ru(3p) spectrum for the alloy was shifted to a higher binding energy by about 1.0 eV relative to that from elemental Ru which could be thought as direct evidence for an electron transfer from Ru in the alloy. Deng's group [39] also studied the surface electronic characteristics of Ni–B and found the binding energy of elemental boron in the Ni–B positively shifted about 1.1 eV, indicating that the boron donated partial electrons to the alloying nickel. Furthermore, the Au $4f_{7/2}$ binding energy of an Au/MoO_x sample was significantly smaller (82.9 eV) than that of the bulk gold film (84.0 eV). Xu [40] considered that the −1.1 eV negative shift of the binding energy of Au $4f_{7/2}$ should be the result of electron transfer from oxygen vacancy sites. Based on the above discussion, the blue shift of Cu $2p_{3/2}$ and unchanged Ti $2p_{3/2}$ (which should be blue shift too) binding energy in the Cu/SiO_2–TiO_2 catalyst could be thought as the result of the electron transfer from Ti to Cu.

However, the role of silica cannot be ignored. Silica provides a relatively large specific surface area for the catalyst, enhances the dispersion of the copper species. In addition, intermediate oxygen

Table 2
Surface Cu component of the reduced catalysts based on Cu LMM deconvolution.

Catalyst	KE (eV)[a]		AP (eV)[b]		$BE_{Cu2p3/2}$[c] (eV)	Cu^0/Cu^{1+}[d] (mol/mol)
	Cu^0	Cu^+	Cu^0	Cu^+		
Cu/SiO_2	918.8	916.2	1850.8	1848.4	932.2	1.5
Cu/TiO_2	918.6	916.1	1851.2	1848.8	932.6	1.2
Cu/SiO_2–TiO_2	918.6	916.1	1850.7	1848.2	932.0	1.9

[a] Kinetic energy.
[b] Auger parameter.
[c] Binding energy of the reduced samples.
[d] $Cu^0/(Cu^+) \times 100\%$.

atoms in the Si—O—Ti bonds can further facilitate the electron activation in the TiO_2 [41,42]. Both the reducibility and the surface charge density of the copper species are enormously enhanced by the electron transfer between copper and the Ti–Si binary-oxide support. This conclusion is in accordance with the result from the X-ray induced Auger spectra (XAES) Cu LMM as shown in Fig. 6. Two overlapping Cu LMM XAES peaks at about 918.6 and 916.2 eV can be observed obviously, indicating that Cu^0 and Cu^{1+} co-exist in the reduced catalysts. The modified Auger parameter α is another indicator to identify the chemical state of copper species. Deconvolution of the original spectra and the peak positions as well as their contributions extracted from the deconvolution are listed in Table 2. The Auger parameter of copper varying from 1848.2 to 1849.8 eV certifies the existence of Cu^{1+} among the metallic copper species. It is also found that the amount of metallic copper species on the Cu/SiO_2–TiO_2 sample is more than that of the other two samples. This finding can be considered as another evidence to demonstrate that using the binary oxide support can enhance the reducibility of copper oxide species and create more active sites during the catalytic reaction. It should be noted that the ratio of Cu^0/Cu^{1+} did shift to lower value after 30 h reaction, especially for the unitary oxide supported catalyst, indicating that the metallic copper species played an important role in the hydrogenation process.

3.4. Catalytic activities

Hydrogenation of DMO to EG is used as a probe reaction under the optimized condition to investigate the relationship between the catalytic performance and the intrinsic structure of the catalysts. This hydrogenation reaction is a two-step tandem catalytic reaction: firstly, hydrogenation of DMO to methylglycollate (MG); secondly, hydrogenation of MG to EG, the target product. Other by-products such as ethanol (hydrogenation product from EG) and 1,2-butanediol (generated by the strong acid sites) are not detected in our reaction. Fig. 7 displays that the conversion of DMO can

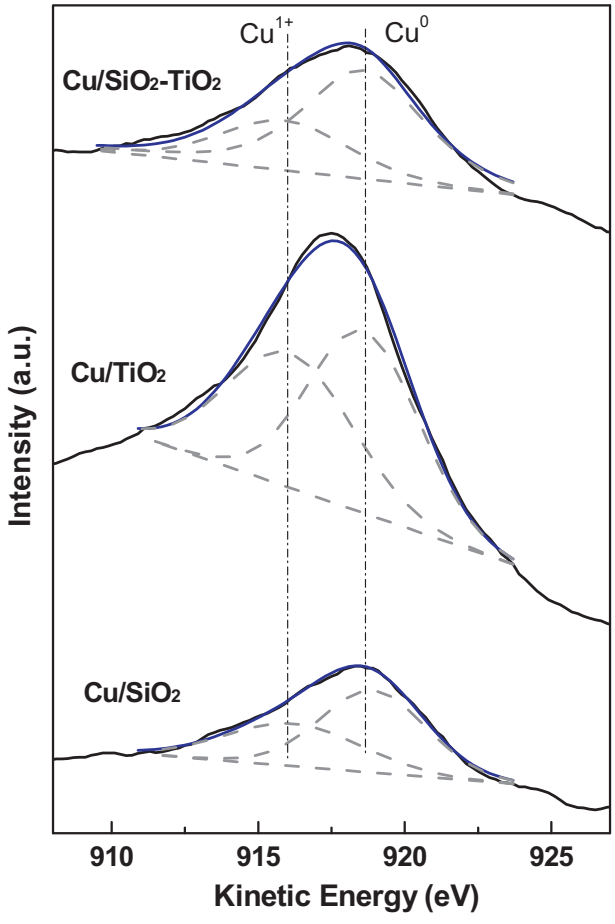

Fig. 6. Cu LMM XAES spectra of the reduced catalysts at 573 K.

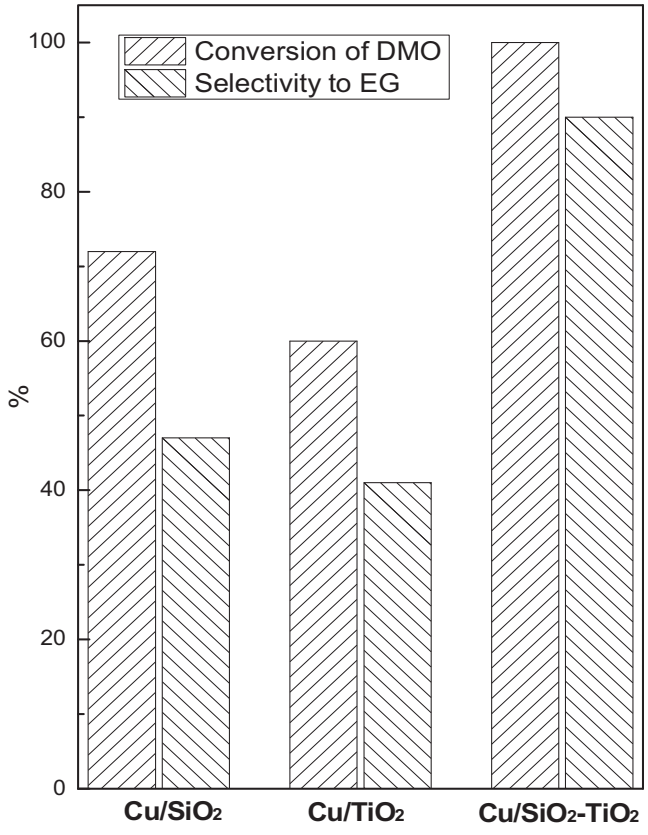

Fig. 7. Catalytic performance of the catalysts. Reaction condition: $P = 3$ MPa, $T = 473$ K, H_2/DMO = 100 (mol/mol), LHSV = 0.6 h^{-1}.

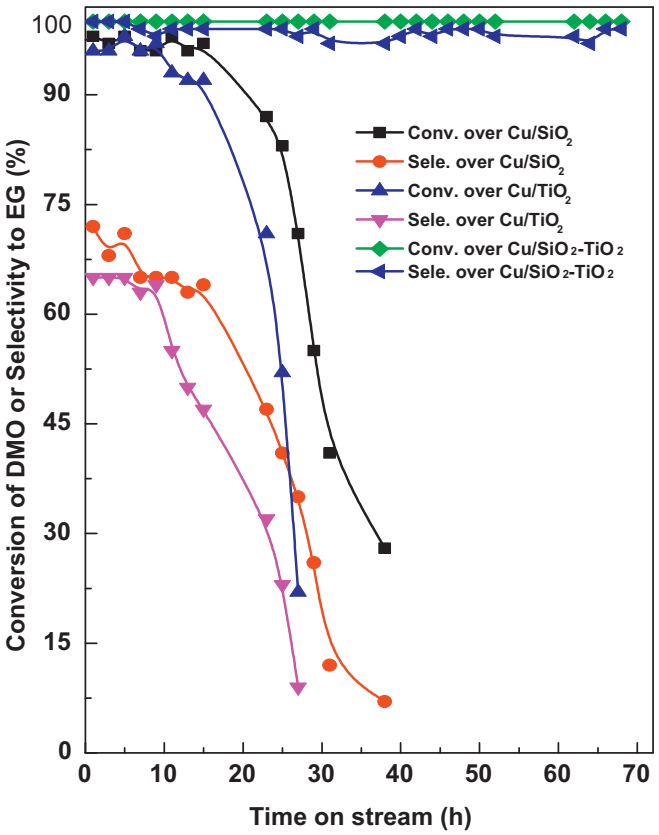

Fig. 8. Stability test of the catalysts. Reaction condition: $P = 3$ MPa, $T = 473$ K, H_2/DMO = 100 (mol/mol), LHSV = 0.3 h^{-1}.

reach 100% when the Si–Ti binary oxide are used as the support, and the selectivity to EG can reach 90% even at a relatively high LHSV, 0.6 h^{-1}. By contrast, both the conversion and selectivity of Cu/SiO_2 and Cu/TiO_2 were relatively low. The main product for the two catalysts is MG. In the Cu/SiO_2 sample, because of the weak interaction of the copper species and silica, copper species tend to aggregate into large particles easily and exhibited poor activity and stability [11,16,43,44]. For the Cu/TiO_2 catalyst, the low BET surface area of the catalyst further restrains the contact between the active sites and the reactants; additionally, the poor reducibility of the copper species in the Cu/TiO_2 catalyst could also be responsible for the low activity. For the Cu/TiO_2–SiO_2 catalyst, the beneficial influence of the TiO_2 and the large metallic Cu surface area could be obtained and further lead to a remarkable enhancement for the catalytic performance.

To investigate the long-term stability of the catalysts, the life test (Fig. 8) was carried out at 473 K with LHSV at 0.3 h^{-1}. It is clear that the obvious deactivation of Cu/SiO_2 and Cu/TiO_2 begin from 23 to 11 h, respectively, the selectivity to EG decreases drastically and the partial hydrogenation product, MG, becomes the main product. Generally, once MG is generated and becomes the main product for the copper catalyst, the deactivation of catalyst will occur. However, the conversion of DMO and selectivity to EG for the Cu/SiO_2–TiO_2 catalyst still stay above 97% even after 70 h time on stream without decrease of selectivity to EG, suggesting its super stability as compared with the other two counterparts. In addition, the catalytic activity test was also carried out on the other Si–Ti binary oxide supported catalyst with higher copper loading (25 wt.%), and both the conversion and selectivity to EG were still constant even after 300 h at LHSV of 0.6 h^{-1} which were greatly higher than those over Cu/SiO_2 and Cu/TiO_2 catalysts.

4. Discussions

The outstanding catalytic hydrogenation performance and long-term stability could be obtained via the Si–Ti binary oxide supported catalyst. The structural and textural evolution analysis reveals that the introduction of TiO_2 into the SiO_2 support not only could improve the dispersion of active copper species, but also could strengthen the interaction between the copper species and binary oxide supports. The binary oxide supported copper catalyst made full use of large specific surface area provided by SiO_2 and strong interaction between copper species and TiO_2. Although it is generally accepted that the stronger interaction between copper and the supports may lead to better copper dispersion, thus, the TiO_2 support may facilitate the copper distribution better than the SiO_2 support, however, the aggregation of the copper species does occur on the TiO_2 support, which might be attributed to the small specific surface area of the TiO_2. The TEM image of Cu/SiO_2–TiO_2 and Cu/SiO_2 indicates that the textural properties are similar for the two catalysts. The hydrogen consumption at lower temperature based on the TPR characterization in the binary oxide supported catalysts could be ascribed to the electron transfer from the TiO_2 to Cu, which could be further confirmed by the XPS results.

Numerous studies indicate that metallic copper species play an important role in the hydrogenation of esters. Metallic copper species with strong hydrogen activating capacity are considered as active site in the hydrogenation of dimethyl maleate, furfural and crotonaldehyde [45]. Gong's group [46] found that Cu^0 could act as the primary active site to activate H_2 and Cu^+ could facilitate the conversion of the intermediates in the hydrogenation of DMO. Recently we found that tiny amount of cobalt decoration will greatly enhance the catalytic property of the Cu/SiO_2 catalyst [13], and the metallic cobalt species will enormously promote the hydrogen activation process. Our result also confirms that the hydrogen activation is extremely important to the hydrogenation of DMO to EG. It is generally accepted that the synergistic effect of Cu^0 and Cu^+ determines the catalytic performance in the hydrogenation of DMO to EG. However, the proper ratio of Cu^0/Cu^+ in the working catalyst still seems undefined. Chen et al. [27] studied the Cu/SiO_2 catalyst and found that the Cu/SiO_2 with the maximal ratio of $Cu^+/(Cu^0 + Cu^+)$ displayed the best catalytic activity. In the series of boron doped Cu/SiO_2 catalysts studied by Yuan's group [44], the surface Cu^+ concentration increased with introduction amount of boron to the Cu/SiO_2, however, the catalytic performance increased first and then decreased with the higher Cu^+ concentration in the catalyst.

Our previous study on the Cu/SiO_2 catalyst prepared with different initial precipitation temperature showed that the CS-60 catalyst with highest ratio of Cu^0/Cu^{1+} had the best catalytic performance [11]. It's important to note that, other experimental parameters such as metal loading, pretreatment process, and reaction condition will inevitably impact on the catalytic performance. In our research, we find that the Si–Ti binary oxide support hosts highly dispersed Cu nanoparticles, which could provide more active sites for hydrogenation of DMO. Both the XPS and TPR measurements evidence the electron transfer between copper and the supports. The electrons transfer from the TiO_2 to Cu are just analogous to the charge-density effect on Cu caused by the electronic modulation of ZnO support [21,47]. Liao et al. found that the Cu phase with the electronic promotion on the interface could assist CO_2 molecular rearrangement and hydrogenation to give methanol. Based on these discussions, the negative charges on the metallic copper surface in the Cu/SiO_2–TiO_2 could promote the carbonyl group adsorption and further enhance the catalytic performance. Furthermore, the high concentration of the metallic copper on the surface of the catalyst will enormously facilitate the hydrogen activation and provide more active hydrogen to react with the DMO molecules

which could remarkably enhance the catalytic properties even at higher LHSV.

For the copper-based catalysts, the dispersion of the copper species on the supports is of great importance for the catalytic stability. Gong' group studied the boron-modified silica supported copper catalysts and found that when boron was incorporated into the catalyst, the generated defects promoted the dispersion of copper species. Additionally, the strong interaction between boric oxide and surface cupreous species could possibly retard the surface transmigration of copper nanoparticles during the high-temperature heat treatment, leading to excellent catalytic stability [16]. Compared to the Cu/SiO_2 or Cu/TiO_2, the high specific surface area of the support in the Cu/SiO_2–TiO_2 catalyst and the moderate interaction between copper and the supports will greatly improve the dispersion of the copper species, which could further lead to high copper surface area and enhance the catalytic performance.

5. Conclusions

In summary, a novel copper based catalyst with Si–Ti binary oxide support displays high catalytic activity and long stability in the hydrogenation of DMO to EG. The beneficial influence of TiO_2 and better copper dispersion could be obtained by using Si–Ti binary oxide support compared to the unitary SiO_2 or TiO_2 support. The electrons transfer from TiO_2 to the copper species could enhance the copper reducibility and cause more negative charges on the metallic copper surface which may facilitate the hydrogen activation and help to promote the catalytic performance. This approach of using the binary oxide as support to load copper may gain some new insights into the hydrogenation of DMO to EG process and guidance significance for its further industrial applications.

Acknowledgments

We thank the Major State Basic Resource Development Program (Grant No. 2012CB224804), NNSFC (Project 21173052, 20903035), and the Science & Technology Commission of Shanghai Municipality (08DZ2270500) for financial support.

References

[1] H. Yue, Y. Zha, X. Ma, J. Gong, Chem. Soc. Rev. 41 (2012) 4218–4244.
[2] S. Rebsdat, D. Mayer, Ullmann's Encyclopedia of Industrial Chemistry, Wiley-VCH Verlag GmbH & Co. KGaA, Weinheim, 2000, 531.
[3] D.S. Brands, E.K. Poels, A. Bliek, Appl. Catal. A-Gen. 184 (1999) 289–297.
[4] H. Kobayashi, N. Takesawa, C. Minochi, J. Catal. 69 (1981) 487–494.
[5] T. Sodesawa, M. Nagacho, A. Onodera, F. Nozaki, J. Catal. 102 (1986) 460–463.
[6] S. Sitthisa, T. Sooknoi, Y. Ma, P.B. Balbuena, D.E. Resasco, J. Catal. 227 (2011) 1–13.
[7] S. Wang, X. Li, Q. Yin, L. Zhu, Z. Luo, Catal. Commun. 12 (2011) 1246–1250.
[8] H. Xie, J.Y. Howe, V. Schwartz, J.R. Monnier, C.T. Williams, H.J. Ploehn, J. Catal. 259 (2008) 111–122.
[9] D.S. Brands, E.K. Poels, A. Bliek, Appl. Catal. A-Gen. 184 (1999) 279–289.
[10] T. Susumu, F. Kozo, N. Keigo, M. Masaoki, M. Katsuhiko, EP 0046983, 1982.
[11] A. Yin, X. Guo, K. Fan, W.L. Dai, Catal. Commun. 12 (2011) 412–416.
[12] A. Yin, X. Guo, K. Fan, W.L. Dai, ChemCatChem 2 (2010) 206–213.
[13] C. Wen, Y. Cui, A. Yin, K. Fan, W.L. Dai, ChemCatChem 5 (2013) 138–141.
[14] A. Yin, X. Guo, W.L. Dai, K. Fan, J. Phys. Chem. C 113 (2009) 11003–11013.
[15] A. Yin, C. Wen, X. Guo, W.L. Dai, K. Fan, J. Catal. 280 (2011) 77–88.
[16] S. Zhao, H. Yue, Y. Zhao, L. Zhao, B. Wang, J. Lv, S. Wang, J. Gong, X. Ma, J. Catal. 297 (2013) 142–150.
[17] H. Irie, S. Miura, K. Kamiya, K. Hashimoto, Chem. Phys. Lett. 457 (2008) 202–205.
[18] H. Irie, K. Kamiya, T. Shibanuma, S. Miura, D.A. Tryk, T. Yokoyama, K. Hashimoto, J. Phys. Chem. C 113 (2009) 10761–10766.
[19] Y. Kanai, T. Watanabe, T. Fujitani, T. Uchijima, J. Nakamura, Catal. Lett. 38 (1996) 157–163.
[20] J. Nakamura, I. Nakamura, T. Uchijima, Y. Kanai, T. Watanabe, M. Saito, T. Fujitani, J. Catal. 160 (1996) 65–75.
[21] F. Liao, Y. Huang, J. Ge, W. Zheng, K. Tedsree, P. Collier, X. Hong, S.C. Tsang, Angew. Chem. Int. Ed. 50 (2011) 2162–2165.
[22] Z. Ding, H.Y. Zhu, P.F. Greenfield, G.Q. Lu, J. Colloid Interface Sci. 238 (2001) 267–272.
[23] D. Volkmer, S. Tugulu, M. Fricke, T. Nielsen, Angew. Chem. Int. Ed. 42 (2003) 58–61.
[24] F. Boccuzzi, S. Coluccia, G. Martra, N. Ravasio, J. Catal. 184 (1999) 316–326.
[25] F. Boccuzzi, G. Martra, C.P. Papalia, N. Ravasio, J. Catal. 184 (1999) 327–334.
[26] H. Yue, Y. Zhao, L. Zhao, J. Lv, S. Wang, J. Gong, X. Ma, AIChE 58 (2012) 2798–2809.
[27] L.F. Chen, P.J. Guo, M.H. Qiao, S.R. Yan, H.X. Li, W. Shen, H.L. Xu, K.N. Fan, J. Catal. 257 (2008) 172–180.
[28] L. Gu, F. Song, N.W. Zhu, Appl. Catal. B-Environ. 101 (2011) 431–440.
[29] W.S. Xia, Y.H. Hou, G. Chang, W.Z. Weng, Int. J. Hydrogen Energy 37 (2012) 8343–8353.
[30] S. Wang, G. Sun, Z. Wu, Q. Xin, J. Power Sources 165 (2007) 128–133.
[31] A.J. Marchi, J. Fierro, J. Santamaría, A. Monzón, Appl. Catal. A-Gen. 142 (1996) 375–386.
[32] F.W. Chang, H.C. Yang, L.S. Roselin, W.Y. Kuo, Appl. Catal. A-Gen. 304 (2006) 30–39.
[33] H. Zhu, Y. Wu, X. Zhao, H. Wan, L. Yang, J. Hong, Q. Yu, L. Dong, Y. Chen, C. Jian, J. Mol. Catal. A-Chem. 243 (2006) 24–30.
[34] P.W. Wang, L. Zhang, J. Non-Cryst. Solids 194 (1996) 129–134.
[35] Y.D. Hou, X.C. Wang, L. Wu, X.F. Chen, Z.X. Ding, X.X. Wang, X.Z. Fu, Chemosphere 72 (2008) 414–421.
[36] R.N. Viswanath, S. Ramasamy, Colloids Surf. A 133 (1998) 49–56.
[37] J. Panpranot, K. Kontapakdee, P. Praserthdam, Appl. Catal. A-Gen. 314 (2006) 128–133.
[38] J. Goodenough, R. Manoharan, Chem. Mater. 1 (1989) 391–398.
[39] H. Li, H. Li, W.L. Dai, W. Wang, Z. Fang, J.F. Deng, Appl. Surf. Sci. 152 (1999) 25–34.
[40] F. Wang, W. Ueda, J. Xu, Angew. Chem. Int. Ed. 51 (2012) 3883–3887.
[41] J. Ren, S. Liu, Z. Li, K. Xie, Catal. Commun. 12 (2010) 357–361.
[42] J. Ren, S. Liu, Z. Li, X. Lu, K. Xie, Appl. Catal. A-Gen. 366 (2009) 93–101.
[43] J. Lin, X. Zhao, Y. Cui, H. Zhang, D.W. Liao, Chem. Commun. 48 (2012) 1177–1179.
[44] Z. He, H. Lin, P. He, Y. Yuan, J. Catal. 277 (2011) 54–63.
[45] M. Mokhtar, C. Ohlinger, J.H. Schlander, T. Turek, Chem. Eng. Technol. 24 (2001) 423–426.
[46] J. Gong, H. Yue, Y. Zhao, S. Zhao, L. Zhao, J. Lv, S. Wang, X. Ma, J. Am. Chem. Soc. 134 (2012) 13922–13925.
[47] F. Liao, Z. Zeng, C. Eley, Q. Lu, X. Hong, S.C. Tsang, Angew. Chem. Int. Ed. 124 (2012) 5934–5938.